Rotational analysis of the BaI $C^2\Pi - X^2\Sigma^+$ (0, 0) band

MARK A. JOHNSON,[1] CHIFURU NODA, JOHN S. MCKILLOP, AND RICHARD N. ZARE[2]
Department of Chemistry, Stanford University, Stanford, CA 94305, U.S.A.

Received June 6, 1984

Rotational analysis of the BaI $C^2\Pi - X^2\Sigma^+$ (0, 0) band system has been performed using molecular beam and laser spectroscopic techniques. This band is free from local perturbations, although significant interaction of the $C^2\Pi$ state with several other $^2\Sigma^+$ states is indicated. The spin-orbit ordering of the C state is confirmed to be regular, while the Λ-doubling parameters p and q are opposite in sign. Apparent anomalies in the line strengths of various rotational branches in the two spin-orbit sub-bands are related to observed differences in the hyperfine structure of the C-state spin-orbit components.

On a effectué une analyse rotationnelle du système de bandes $C^2\Pi - X^2\Sigma^+$ (0, 0), en utilisant des techniques de faisceaux moléculaires et de spectroscopie laser. Cette bande est exempte de perturbations locales, bien qu'elle présente des signes d'une interaction importante de l'état $C^2\Pi$ avec plusieurs autres états $^2\Sigma^+$. La régularité de l'ordre spin-orbite de l'état C est confirmée, alors que les paramètres p et q du doublement Λ sont de signes opposés. Les anomalies apparentes de l'intensité des raies de diverses branches rotationnelles dans les deux sous-bandes spin-orbite sont reliées aux différences observées dans la structure hyperfine des composantes spin-orbite de l'état C.

[Traduit par le journal]

Can. J. Phys. 62, 1467 (1984)

1. Introduction

Often the question is raised as to whether lasers are truly a revolution in spectroscopy or whether they represent instead answers in search of new questions. Certainly for the study of very high resolution spectra, such as the measurement of hyperfine splittings, laser methods are often essential to reveal features otherwise hidden in the Doppler line profile. It is less obvious, on the other hand, that laser techniques compete as effectively with the traditional photographic plate techniques so elegantly practiced by Herzberg and others (1), especially when one is rotationally analyzing optical band systems in which sub-Doppler methods are not required.

Clearly in some cases, such as NO_2, where the rotational structure of the band is open but not regular, traditional methods can be powerfully augmented by laser techniques such as dispersed laser-induced fluorescence (LIF), which simplifies the assignment procedure (2). In this paper, we are concerned with the $C^2\Pi - X^2\Sigma^+$ band system of the diatomic molecule BaI, centered at approximately 5500 Å (3–6). This system presents a different challenge to traditional spectroscopic approaches, that of extremely congested rotational structure due to the exceedingly high line density present in this band system. This congestion results not only from the very small rotational constant of such a heavy molecule, but also from extensive overlapping of vibrational sequences, and spin-rotation doubling, Λ doubling, and hyperfine splitting of the rotational levels involved.

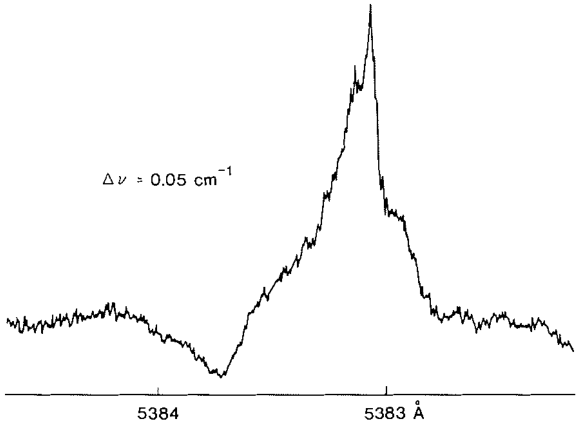

FIG. 1. An excitation spectrum of the $C^2\Pi_{3/2} - X^2\Sigma^+$ (0, 0) band of BaI taken using a molecular beam source and a laser bandwidth of 0.05 cm^{-1}.

The problems inherent in the analysis of the BaI $C-X$ band are illustrated in Fig. 1, which presents an excitation spectrum of the (0, 0) band taken using a molecular beam source and a laser bandwidth of approximately 0.05 cm^{-1}, comparable to the Doppler width obtained in flame sources operating around 600 K. No isolated rotational features can be seen at this bandwidth, completely precluding a satisfactory rotational analysis. The line density to the blue side of the origin exceeds 200 lines/cm^{-1} (excluding hyperfine transitions) so that BaI presents an interesting case in which sub-Doppler techniques, usually reserved for the study of hyperfine structure, must now be employed

---

[1] Present address: Joint Institute for Laboratory Astrophysics, University of Colorado, Boulder, CO 80309 U.S.A.

[2] Holder of a Shell Distinguished Chair.

just to observe the rotational structure of the band.

To obtain an assignment of the $C-X$ band, we employed a novel version of the optical–optical double resonance technique that takes advantage of the phase relationships between double resonance transitions having either upper or lower rotational states in common with a particular "labeled" rotational transition (6). This task was simplified even further owing to the reduction of the Doppler widths afforded by performing the double resonance experiment on a collimated molecular beam of BaI. In this paper we present the spectroscopic data obtained by analysis of our previous measurements and report the spectroscopic constants that result from the reduction of the data.

Prior to this study, analysis of the BaI visible spectrum has been restricted to band head measurements, first by Walters and Barratt (4) and later refined by Patel and Shah (5).[3] Also, the overlapping $A^2\Pi - X^2\Sigma^+$ and $B^2\Sigma^+ - X^2\Sigma^+$ systems have been found by Bradford *et al.* (7) and are observed to lie approximately 10 000 cm^{-1} above the ground state. The location of the lowest $^2\Delta$ state is still unknown, although a $^2\Delta$ state has recently been found for BaCl and it lies below the $A^2\Pi$ state (8). The $C^2\Pi - X^2\Sigma^+$ band is of particular interest, since issues concerning the molecular orbital structure of alkaline earth monohalides hinge on the values of Λ-doubling and hyperfine parameters in the C state. Such detailed information is not presently available for any alkaline earth-monohalide $C^2\Pi$ states, although the rotational constants, B_0 and D_0, have been reported for the CaCl $C^2\Pi$ state (9). We present here assignments of over 400 rotational transitions within the $C-X$ (0, 0) band and report for the first time a set of rotational constants for the BaI C and X states.

2. Experimental

The optical–optical double resonance (OODR) assignment methods and experimental apparatus are described in an earlier publication (6). Additional details of the OODR methods used here will be presented in a forthcoming publication (Johnson and Zare, manuscript in preparation). Briefly, BaI was formed in a molecular beam by heating Ba and BaI$_2$ in a stainless steel crucible to approximately 1300 K. The beam was then collimated to yield Doppler widths between 20 and 150 MHz, depending on the particular experimental needs. Single-mode continuous wave (CW) dye lasers (Coherent 599-21) operating with rhodamine 110 provided a power of approximately 50 mW in each sub-band for double resonance spectra, while lower powers (~10 mW) were used for high-resolution excitation spectra to reduce the effects of power broadening. Frequency measurements of rotational transitions assigned via double resonance were then obtained by measurement of line centers from the excitation spectra, using fringes from a 300-MHz etalon to interpolate between frequencies of I$_2$ reference lines (10). This provided a measurement accuracy of ~±0.002 cm^{-1}.

Additional assignments within a few rotational branches were provided in two ways. Owing to large differences in the hyperfine structure of rotational branches in the $C^2\Pi_{1/2} - X^2\Sigma^+$ sub-band discussed below, progressions in both the Q_1- and Q_{12}-branches were easily identified. Thus, once the double resonance assignments were made for a few transitions in these branches, it was possible to immediately assign more than 70 lines in each.

The analogous extensions of the OODR assignments in the R_1- and P_{12}-branches were carried out by applying selectively detected laser-induced fluorescence (SDLIF) (11) to the BaI molecular beam. In this case an Interactive Technology 3/4-m monochromator with 150-μm slits was used to isolate fluorescence in the $Q_1 + R_{12}$ ($P_1 + Q_{12}$)-branches, which results from excitation of transitions in the P_{12} (R_1)-branch. Scanning the excitation laser through the P_{12} (or R_1)-branch thus produces the SDLIF spectrum of that branch, as illustrated in Fig. 2. Standard photon counting techniques were used, with the analog signal obtained from a rate meter displayed on an $x-y$ recorder. With this arrangement, count rates on the peak of BaI transitions were on the order of 300 counts/s.

3. Results

3.1 Appearance of the spectrum

The vibrational structure of the $C^2\Pi - X^2\Sigma^+$ band is dominated by two sub-bands (5), $C^2\Pi_{1/2} - X^2\Sigma^+$ at 5612 Å and $C^2\Pi_{3/2} - X^2\Sigma^+$ at 5383 Å, hereafter referred to as C_1-X and C_2-X, respectively. Only the $\Delta v = 0$ sequences are observed at low v ($v < 10$), and both sub-bands appear identical at low resolution (~1 cm^{-1}), showing band heads of the $\Delta v = 0$ sequences evenly separated by about 6.1 cm^{-1}. At low v, the band heads are formed shaded to the red side opposite to the behavior observed at high v ($v > 25$) where the heads are shaded to the blue side (12). Analysis of these band heads has been performed by other workers up to high vibrational levels in the $C-X$ band (4, 5). However, extrapolation of band head behavior based on the rotational analysis of the (0, 0) band presented here, in conjunction with detailed LIF studies of reactively formed BaI, has made it possible to correct some of these vibrational assignments (12). These studies have revealed strong evidence for predissociations of the C state and will be presented in a later publication.

As seen in Fig. 1, a clear dip occurs in the (0, 0) band

---

[3] M. M. Patel, private communication.

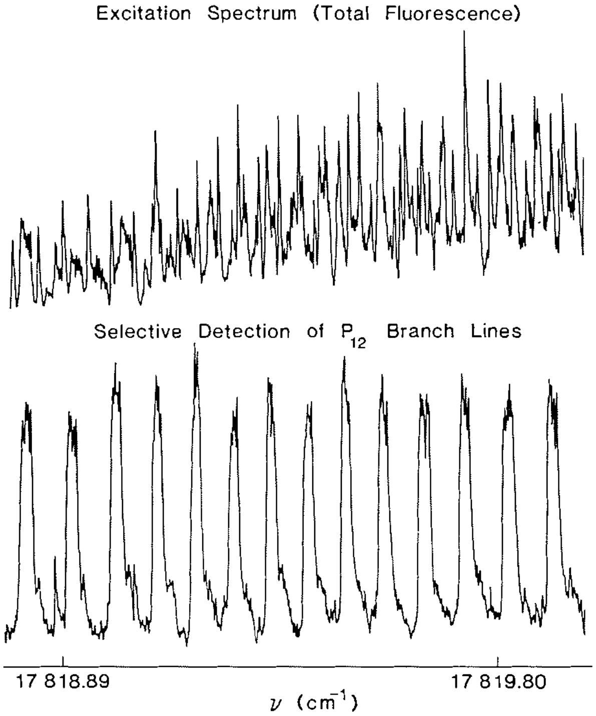

FIG. 2. Selective detection of P_{12}-branch fluorescence observed in a particularly congested region of the $C^2\Pi_{1/2} - X^2\Sigma^+$ band of BaI. The upper trace shows a 30-GHz scan of the excitation spectrum. The lower trace shows individual P_{12}-branch transitions observed when the excitation laser is scanned through this same region in the selective detection experiment. Partially resolved hyperfine structure is apparent in many of the P_{12}-branch transitions.

near the vibronic origin with the band head forming about 2 cm^{-1} to the blue side. Typical 15-GHz segments of the high-resolution, sub-Doppler excitation spectra used in the analysis are shown in Fig. 3. These spectra are centered approximately 4 cm^{-1} to the red side of the origin of each sub-band and are representative of the best resolved regions in each. It should be noted that in many cases observed "lines" are actually blends of two or three rotational transitions. At this resolution (~0.005 cm^{-1}), however, the two spin-orbit sub-bands exhibit qualitatively different excitation spectra. The C_1-X sub-band is dominated by a clear Q_{12}-branch progression, while in the C_2-X sub-band both transitions originating from the $X^2\Sigma^+$ spin-rotation levels (Q_2 and P_{21}) are observed. These Q_2- and P_{21}-branch transitions form an equally characteristic pattern in the C_2-X sub-band, where coincidences in line positions produce a regular "interference" pattern that repeats itself at approximately 1-cm^{-1} intervals.

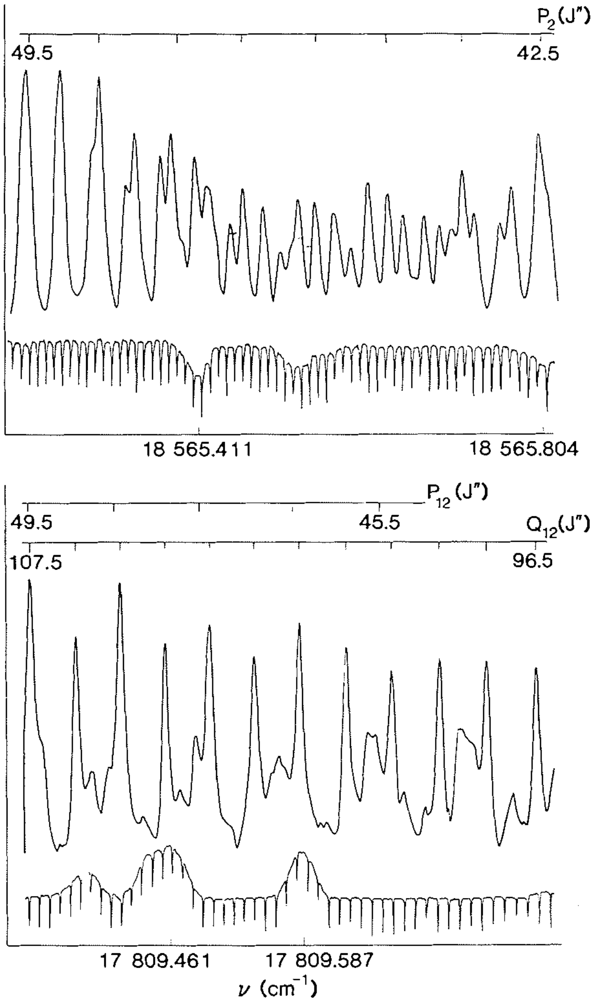

FIG. 3. A comparison of 15-GHz segments of the least congested regions of the $C^2\Pi_{3/2} - X^2\Sigma^+$ (top) and $C^2\Pi_{1/2} - X^2\Sigma^+$ (bottom) (0, 0) band excitation spectra. Both spectra are centered approximately 4 cm^{-1} to the red side of their respective band origins. The corresponding I_2 fluorescence spectrum and 300-MHz etalon fringes used for frequency calibration are included below each spectrum.

Representative SDLIF spectra are shown in Fig. 2, where the upper trace shows a 30-GHz segment of a particularly congested region in the C_1-X sub-band and the lower trace shows the selectively detected P_{12}-branch transitions that are observed when the laser is scanned through this same region in the SDLIF experiment. The structure observed in each P_{12} line is due to partially resolved hyperfine splitting, which has been completely resolved by additional collimation of the molecular beam as shown in Fig. 4. Thus, each P_{12}-branch line is asymmetrically broadened to a total line width on the order of 600 MHz (0.02 cm^{-1}).

Hyperfine structure similar to that in the P_{12}-branch is observed in the P_1- and R_1-branches of the C_1-X sub-band. However, the Q_1- and Q_{12}-branches exhibit

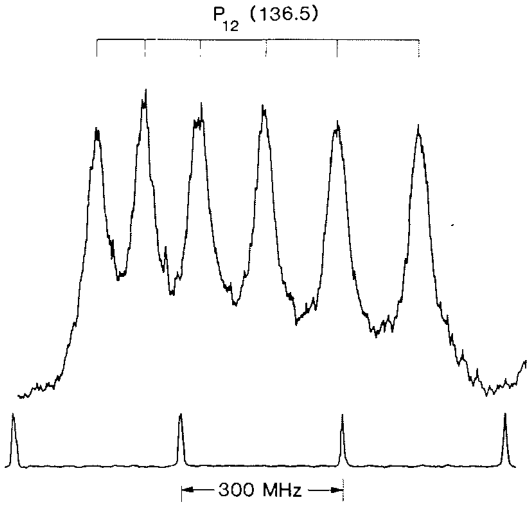

FIG. 4. A Doppler-free, selectively detected excitation spectrum of the P_{12}-(136.5) transition observed using a highly collimated molecular beam of BaI. All six hyperfine components arising from the ^{127}I nuclear spin ($I = 5/2$) are clearly resolved.

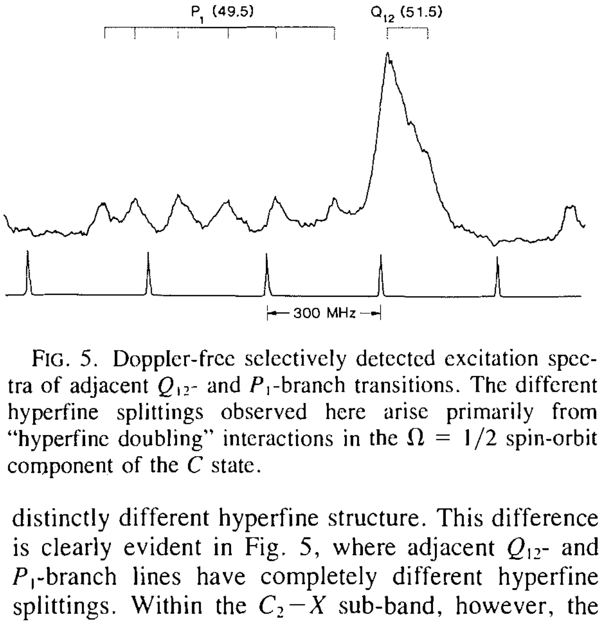

FIG. 5. Doppler-free selectively detected excitation spectra of adjacent Q_{12}- and P_1-branch transitions. The different hyperfine splittings observed here arise primarily from "hyperfine doubling" interactions in the $\Omega = 1/2$ spin-orbit component of the C state.

distinctly different hyperfine structure. This difference is clearly evident in Fig. 5, where adjacent Q_{12}- and P_1-branch lines have completely different hyperfine splittings. Within the C_2-X sub-band, however, the hyperfine structure is essentially identical for all six rotational branches.

The hyperfine problem has been studied in detail and will be treated in a future publication (McKillop, Noda, and Zare, to be published), but several results are relevant to the present discussion. First, the sub-band dependent hyperfine splittings observed here arise from different hyperfine structure within the two spin-orbit components of the C state. The high-J hyperfine splittings observed in the C_2-X transitions arise primarily from the difference between electric quadrupole splittings in the ground and excited states and ground state electron-spin – nuclear-spin interactions. Within the $C^2\Pi_{1/2}$ spin-orbit component, however, additional "hyperfine doubling" interactions introduce parity-dependent hyperfine splittings (13). These result in significant branch dependence of the hyperfine structure in the C_1-X sub-band. The major effect of this is evident in the spectra shown in Fig. 3. The blending of hyperfine components within the Q-branches and large splittings of the hyperfine components within the P- and R-branches of the C_1-X sub-band cause the Q-branch lines to appear even more prominent than one might expect in a normal $^2\Pi$ (case (a)) – $^2\Sigma^+$ transition.

This parity-dependent splitting also introduces asymmetric and branch-dependent shifts in the apparent line centers of these transitions that are significant compared with the line separation within a given branch. In this analysis, the line center was typically taken as the peak or apparent center of a given transition. Thus, it was necessary to correct for the hyperfine offsets in the C_1-X sub-band in order to obtain a set of spectroscopic constants that provide a global fit for the data.

An estimate for this correction was obtained by using the Frosch and Foley parameters (13), resulting from the hyperfine analysis (13), to simulate the overall rotational line profile with a phenomenological Lorentzian line width of ~60 MHz (full width half maximum (fwhm)) for each hyperfine transition. From this simulation it was possible to estimate the apparent line center of the transition and to compare this with the actual center of gravity of the hyperfine multiplet, thus providing an estimate for the hyperfine offset. Owing to problems inherent in such a subjective correction, we estimate that the accuracy of the "line center" measurements reported here are on the order of ± 0.005 cm^{-1}.

The measured line positions (corrected for hyperfine offsets) are collected in the Appendix. Technical difficulties, due to reduced dye efficiency and poorer laser performance in the C_2-X sub-band, resulted in the measurement of only 60 lines in this sub-band, while 369 lines are included in the C_1-X sub-band.

3.2 *Least squares fit*

The line positions were fit to the usual $^2\Pi$ – $^2\Sigma^+$ Hamiltonian using the LINFIT nonlinear least squares program (14). To indicate the overall quality of the fit, the residuals (observed – calculated) are plotted for all rotational branches of each sub-band in Figs. 6 and 7. The standard deviation of the overall fit was 2.00×10^{-3} cm^{-1} and the residuals shown in Figs. 6 and 7 appear free from any serious systematic deviations other than what might be expected owing to problems with the correction for hyperfine offsets. Most line pos-

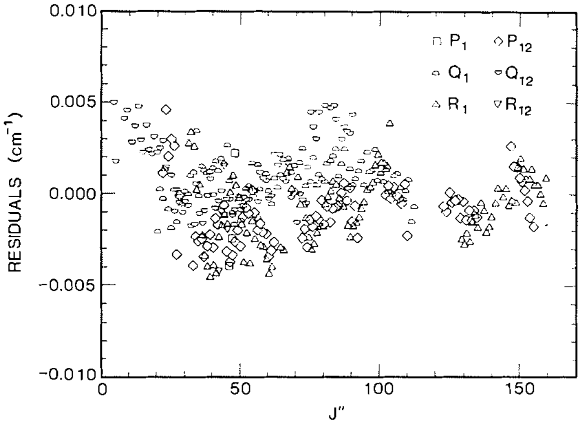

FIG. 6. Residuals between the observed and calculated line positions for the BaI $C^2\Pi_{1/2} - X^2\Sigma^+$ (0,0) band.

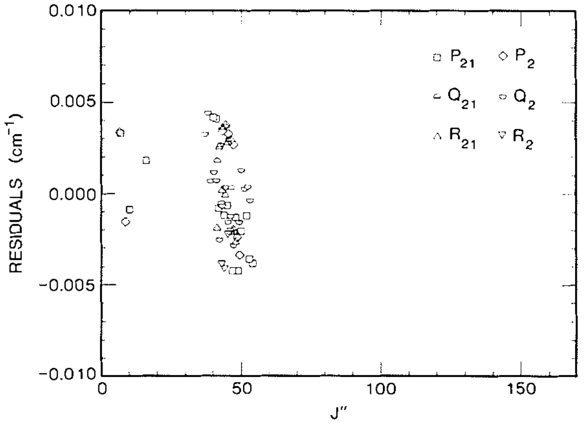

FIG. 7. Residuals between the observed and calculated line positions for the BaI $C^2\Pi_{3/2} - X^2\Sigma^+$ (0,0) band.

TABLE 1. Spectroscopic constants of the BaI $C^2\Pi - X^2\Sigma^+$ (0,0) band (in cm^{-1}). Numbers in parentheses are 2σ uncertainties

ν_0	18 178.310(83)
$A' + o'$	756.10(17)
A'*	782.10(17)
B'	$2.6727(15)\times10^{-2}$
D'	$2.16(19)\times10^{-9}$
o'*	−26.00
p'	$7.107(48)\times10^{-3}$
q'	$-9.6(2.9)\times10^{-5}$
B''	2.67548×10^{-2}
D''	$2.44(19)\times10^{-9}$
γ''	$2.505(21)\times10^{-3}$

*Calculated using pure precession model (see ref. 14).

itions are reproduced to within the standard deviation of the fit, which essentially corresponds to our estimates of the overall measurement uncertainty.

The least squares constants obtained from this fit are collected in Table 1. The removal of any of these constants causes a significant increase in the standard deviation of the fit, while the inclusion of additional parameters (third-order distortion constants, distortion corrections for spin-orbit and Λ-doubling interactions, or phenomenological spin-rotation interactions in the C state) did not significantly decrease the standard deviation of the fit. Thus, the constants presented here should be considered as the minimal data set required to reproduce the experimental line positions.

It should also be pointed out that the spin-orbit coupling constant, A, is totally correlated with the Λ-doubling parameter, o. Thus, only the sum of A and o may be uniquely determined. The value of A reported in Table 1 is estimated using pure precession relations to calculate the value of o. However, pure precession is a poor description for the $C^2\Pi$ state (as will be discussed later). Therefore, great care should be taken when attaching physical meaning to constants determined in such a fit (14).

4. Discussion

4.1 Rotational and centrifugal distortion constants

The observed rotational constants for the $v = 0$ level of the X and C states (0.02675 and 0.02673 cm^{-1}, respectively) are generally in accord with those expected via extrapolation from the other alkali and alkaline earth halides. For instance, the B_0 value of the X state is estimated to be 0.0270 cm^{-1} (12) from bond length extrapolation using trends in the alkali halides and the estimated rotational constant of BaBr (15). The distortion constants are of the same order of magnitude as predicted by the Pekeris relations using the vibrational frequencies of Patel and Shah (5) (2.4×10^{-9} exptl. vs. 3×10^{-9} cm^{-1} calc.)

4.2 Spin splitting of the C *state*

Historically, the marked halogen dependence of the spin-orbit splitting in the BaX C state has caused some uncertainty regarding the nature of its molecular orbital description. Generally this splitting increases from BaF ($A \sim 200$ cm^{-1}) to BaI ($A \sim 750$ cm^{-1}) (16). We observe here, both through the direct probing of the branch origins (6) and through the Λ-doubling behavior, that the C state in BaI is definitely regular, as predicted for a predominantly metal-centered molecular orbital. The CaCl $C^2\Pi$ state was similarly observed to have a regular spin-orbit ordering (9). Thus, a direct mapping of the halogen spin-orbit splitting onto the C state of BaI would not account for the spin-orbit ordering observed here. More detailed information concerning the nature of unpaired electron-spin density in the BaI molecule, especially at the Ba nucleus, will be necessary to clarify the origin of this splitting.

4.3 Λ-Type doubling and spin-rotation splitting

The ground states of MX systems are expected to be largely ionic (M^+X^-) in character with a valence electron occupying a nonbonding orbital centered predominantly on the metal atom (17). Transitions to excited electronic states correspond primarily to the promotion of this nonbonding electron to higher lying nonbonding orbitals that are also metal centered. It has thus been tempting to use pure precession relationships to understand the Λ-doubling, hyperfine, and spin-rotation splittings observed in these systems (18). The pure precession relationships require, however, that the sign of the p and q Λ-doubling parameters be the same for a regular $^2\Pi$ state. Here we find that $p = 7.11\ (\pm\ 0.05) \times 10^{-3}\ \text{cm}^{-1}$ and $q = -9.6\ (\pm 2.9) \times 10^{-5}\ \text{cm}^{-1}$, so that the pure precession relationship does not hold for the case of the BaI C state. Such a situation is not uncommon in the alkaline earth halides, however, and has been observed in the $A^2\Pi$ state of CaI, where the interaction is occurring with a nearby $^2\Sigma^+$ state (19), and in BeF where the $A^2\Pi$ state is regular, while p and q are opposite in sign (20). The failure of pure precession to account for the observed values of p and q indicates that the value of o calculated using these relationships has little physical significance.

Since the spin uncoupling parameter $Y = A/B$ is on the order of 3×10^4 for the C state of BaI, Hund's case (a) behavior is expected to be valid well beyond the highest rotational levels measured here (1). Thus, Λ doubling is anticipated to be more significant in the $\Omega = 1/2$ state than in the $\Omega = 3/2$ state, as is observed. The magnitude of the observed Λ-doubling parameters also suggests significant interaction by one or more $^2\Sigma^+$ states with the $\Omega = 1/2$ component of the C state. Further evidence for such an interaction is provided by the magnitude of the hyperfine doubling interaction in the $C^2\Pi_{1/2}$ state (13), although additional measurements on the X-state hyperfine structure will be required before this can be verified.

While the above discussion of the Λ doubling casts doubt on the validity of applying pure precession relations to the BaI molecule, it is perhaps worth pointing out that the magnitude and sign of the observed spin-rotation constant, γ, in the $X^2\Sigma^+$ state is also not consistent with a pure precession interaction with any known $^2\Pi$ state.

5. Conclusions

The (0, 0) band of the BaI $C^2\Pi - X^2\Sigma^+$ system has been rotationally analyzed using both molecular beam optical–optical double resonance and molecular beam selectively detected laser-induced fluorescence techniques. The spectra are unperturbed and the observed rotational constants (B and D) are essentially the same as predicted by extrapolation from the known behavior of related molecules. The spin-orbit splitting of the C state is regular, as was previously assumed. The Λ-doubling interactions indicate, however, that the $C^2\Pi_{1/2}$ spin-orbit state is strongly interacting with several $^2\Sigma^+$ states. This conclusion is supported by the observed hyperfine structure. More detailed hyperfine studies of this system will be required to establish further the nature of the molecular orbitals involved in the BaI C state, however, and to explain the spin-orbit and Λ-doubling behavior observed in this state.

Acknowledgement

We would like to thank C. R. Webster for his valuable help. We would also like to thank the San Francisco Laser Center for the loan of their equipment. This work was supported by the National Science Foundation under Grant NSF CHE 80-06524 and the Air Force Office of Scientific Research under Grant AFOSR F49620-83-C-0033.

1. G. HERZBERG. Spectra of diatomic molecules. 2nd. ed. D. Van Nostrand Company Inc., New York, NY. 1950.
2. W. DEMTRÖDER. *In* Case studies in atomic physics. Vol. 6. *Edited by* M. R. C. McDowell and E. W. McDaniel. North-Holland Publishing Co., Amsterdam, The Netherlands. 1976.
3. P. MESNAGE. Ann. Phys. (Paris), **12**, 5 (1939).
4. O. H. WALTERS and S. BARRATT. Proc. R. Soc. London Ser. A, **118**, 120 (1928).
5. M. M. PATEL and N. R. SHAH. Indian J. Pure Appl. Phys. **8**, 681 (1978).
6. M. A. JOHNSON, C. W. WEBSTER, and R. N. ZARE. J. Chem. Phys. **75**, 5575 (1981).
7. R. S. BRADFORD, JR., C. R. JONES, L. A. SOUTHALL, and H. P. BROIDA. J. Chem. Phys. **62**, 2060 (1975).
8. H. MARTIN and P. ROYEN. Chem. Phys. Lett. **97**, 127 (1983).
9. E. MORGAN and R. F. BARROW. Nature (London), **185**, 754 (1960).
10. S. GERSTENKORN and P. LUC. Atlas du spectre d'absorption de la molecule d'iode. Centre Nationale de la Recherche Scientifique, Paris, France. 1978; S. GERSTENKORN and P. LUC. Rev. Phys. Appl. **14**, 791 (1979).
11. C. LINTON. J. Mol. Spectrosc. **69**, 351 (1978); M. DULICK, P. F. BERNATH, and R. W. FIELD. Can. J. Phys. **58**, 703 (1980).
12. M. A. JOHNSON. Ph.D. thesis. Stanford University, Stanford, CA. 1983.
13. R. A. FROSCH and H. M. FOLEY. Phys. Rev. **88**, 1337 (1952).
14. R. N. ZARE, A. L. SCHMELTEKOPF, W. J. HARROP, and D. L. ALBRITTON. J. Mol. Spectrosc. **46**, 37 (1973).
15. A. SCHULTZ and A. SIEGEL. J. Mol. Spectrosc. **77**, 235 (1979).

16. K. P. HUBER and G. HERZBERG. Constants of diatomic molecules. D. Van Nostrand Company Inc., New York, NY. 1979.
17. P. J. DAGDIGIAN, H. W. CRUSE, and R. N. ZARE. J. Chem. Phys. **60**, 2330 (1974).
18. P. F. BERNATH. Ph.D. thesis, Massachusetts Institute of Technology, Cambridge, MA. 1980.
19. D. E. REISNER, P. F. BERNATH, and R. W. FIELD. J. Mol. Spectrosc. **89**, 107 (1981).
20. D. L. COOPER, S. J. PROSSER, and W. G. RICHARDS. J. Phys. B, **14**, L487 (1981).

Appendix

Assignments and measured line positions of transitons in the BaI $C^2\Pi - X^2\Sigma^+$ (0, 0) band

J"	P1	P12	Q1	Q12	R1	R12
4.5	----	----	----	17813.117	----	----
5.5	----	----	----	17813.086	----	----
8.5	----	----	----	17812.996	----	----
9.5	----	----	----	17812.969	----	----
11.5	----	----	----	17812.906	----	----
12.5	----	----	----	17812.875	----	----
13.5	----	----	----	17812.844	----	----
14.5	----	----	----	17812.812	----	----
15.5	----	----	----	17812.781	----	----
16.5	----	----	----	17812.750	----	----
17.5	----	----	----	17812.719	----	----
18.5	----	----	----	17812.684	----	----
19.5	----	----	----	17812.652	----	----
20.5	----	----	17813.832	17812.621	----	----
21.5	----	----	17813.859	17812.590	----	----
22.5	----	17811.512	17813.887	17812.559	----	----
23.5	----	17811.434	17813.914	17812.523	----	----
24.5	----	17811.352	17813.937	----	----	----
25.5	----	17811.273	17813.961	17812.457	----	----
26.5	----	17811.195	17813.988	17812.422	----	----
27.5	----	17811.109	17814.012	17812.391	----	----
28.5	----	17811.031	17814.035	17812.355	----	----
29.5	----	----	17814.059	17812.320	----	----
30.5	----	----	17814.086	17812.289	----	----
31.5	----	----	17814.109	17812.254	17815.621	----
32.5	----	----	17814.133	17812.219	17815.691	----
33.5	----	17810.629	17814.156	17812.187	17815.762	----
34.5	----	17810.551	17814.184	17812.152	17815.828	----
35.5	----	17810.469	17814.203	17812.117	17815.898	----
36.5	----	17810.387	17814.230	17812.082	17815.965	----
37.5	----	17810.305	17814.254	17812.051	17816.035	----
38.5	----	17810.227	17814.273	17812.016	17816.102	----
39.5	----	17810.145	17814.297	17811.980	17816.172	----
40.5	----	17810.062	17814.320	17811.945	17816.242	----
41.5	----	17809.980	17814.344	17811.910	17816.309	----
42.5	----	17809.898	17814.367	17811.875	17816.383	17814.492
43.5	----	----	17814.391	17811.840	17816.449	17814.520
44.5	----	17809.738	17814.410	17811.801	17816.520	17814.547
45.5	----	17809.652	17814.434	17811.766	17816.586	17814.566
46.5	17811.648	17809.570	17814.453	17811.730	17816.656	----
47.5	17811.609	17809.488	17814.473	17811.695	17816.727	----

APPENDIX (*Continued*)

J"	P1	P12	Q1	Q12	R1	R12
48.5	17811.574	17809.406	17814.496	17811.656	17816.793	----
49.5	----	17809.324	17814.520	17811.621	17816.859	----
50.5	----	17809.238	17814.539	17811.586	17816.926	----
51.5	----	17809.160	17814.559	17811.551	17816.992	----
52.5	----	17809.074	17814.582	17811.512	17817.062	----
53.5	----	17808.992	17814.602	17811.477	17817.129	----
54.5	----	17808.910	17814.625	17811.437	17817.195	----
55.5	----	17808.824	17814.645	17811.402	17817.262	----
56.5	----	17808.742	17814.664	17811.363	17817.332	----
57.5	----	17808.656	17814.684	17811.328	17817.395	----
58.5	----	17808.574	17814.707	17811.289	17817.461	----
59.5	----	17808.488	17814.727	17811.250	17817.527	----
60.5	----	17808.402	17814.746	17811.211	17817.594	----
61.5	----	17808.320	17814.766	17811.176	17817.660	----
62.5	----	17808.234	17814.785	17811.137	----	----
63.5	----	----	17814.805	17811.098	----	----
64.5	----	----	17814.824	17811.062	17817.855	----
65.5	----	----	17814.844	17811.020	17817.922	----
66.5	----	----	17814.863	17810.980	17817.992	----
67.5	----	----	17814.883	17810.945	17818.059	----
68.5	----	----	17814.898	17810.902	17818.121	----
69.5	----	----	17814.918	17810.863	17818.187	----
70.5	----	----	17814.937	17810.824	17818.250	----
71.5	----	----	17814.957	17810.785	17818.316	----
72.5	----	17807.383	17814.977	17810.746	17818.379	----
73.5	----	17807.297	17814.992	17810.703	17818.441	----
74.5	----	17807.211	17815.012	----	17818.504	----
75.5	----	17807.125	17815.027	17810.629	17818.570	----
76.5	----	17807.039	17815.047	17810.590	17818.633	----
77.5	----	17806.953	17815.062	17810.547	17818.699	----
78.5	----	17806.863	17815.078	17810.508	17818.762	----
79.5	----	17806.781	17815.098	----	17818.824	----
80.5	----	17806.691	17815.113	17810.430	17818.891	----
81.5	----	17806.605	17815.133	17810.387	17818.953	----
82.5	----	17806.516	17815.148	17810.348	17819.016	----
83.5	----	17806.430	17815.164	17810.305	17819.078	----
84.5	----	17806.344	17815.184	17810.262	17819.141	----
85.5	----	17806.258	17815.199	----	17819.203	----
86.5	----	17806.168	17815.215	17810.180	17819.266	----
87.5	----	17806.082	17815.230	17810.137	17819.328	----
88.5	----	17805.992	17815.246	17810.098	17819.391	----

APPENDIX (*Continued*)

J"	P1	P12	Q1	Q12	R1	R12
89.5	----	17805.906	17815.262	17810.055	17819.449	----
90.5	----	17805.816	17815.277	17810.012	17819.512	----
91.5	----	17805.730	17815.293	----	17819.574	----
92.5	----	17805.637	17815.309	----	17819.637	----
93.5	----	----	17815.324	----	17819.699	----
94.5	----	----	17815.340	----	17819.762	----
95.5	----	----	17815.355	----	17819.820	----
96.5	----	----	17815.371	----	17819.883	----
97.5	----	----	17815.387	----	17819.945	----
98.5	----	----	17815.402	----	17820.008	----
99.5	----	----	17815.414	----	17820.066	----
100.5	----	----	17815.430	----	17820.129	----
101.5	----	----	17815.445	----	17820.187	----
102.5	----	17804.750	17815.461	----	17820.250	----
103.5	----	17804.664	17815.473	----	17820.312	----
104.5	----	17804.570	17815.484	----	----	----
105.5	----	17804.484	17815.500	----	----	----
106.5	----	17804.395	17815.516	----	----	----
107.5	----	17804.301	17815.527	----	----	----
108.5	----	17804.211	17815.539	----	----	----
109.5	----	17804.125	17815.555	----	----	----
110.5	----	17804.031	17815.570	----	----	----
111.5	----	----	17815.578	----	----	----
112.5	----	----	17815.594	----	----	----
123.5	----	17802.848	----	----	----	----
124.5	----	17802.758	----	----	----	----
125.5	----	17802.668	----	----	----	----
126.5	----	17802.574	----	----	----	----
127.5	----	17802.480	----	----	----	----
128.5	----	17802.391	----	----	----	----
129.5	----	17802.297	----	----	17821.824	----
130.5	----	17802.207	----	----	17821.883	----
131.5	----	17802.113	----	----	17821.937	----
132.5	----	17802.020	----	----	17821.996	----
133.5	----	17801.930	----	----	17822.055	----
134.5	----	17801.836	----	----	17822.109	----
135.5	----	17801.742	----	----	17822.164	----
136.5	----	----	----	----	17822.223	----
137.5	----	----	----	----	17822.277	----
138.5	----	----	----	----	17822.332	----
139.5	----	----	----	----	17822.391	----
140.5	----	----	----	----	17822.445	----

APPENDIX (*Concluded*)

J"	P1	P12	Q1	Q12	R1	R12
141.5	----	----	----	----	17822.504	----
142.5	----	----	----	----	17822.559	----
144.5	----	----	----	----	17822.668	----
145.5	----	----	----	----	17822.727	----
146.5	----	----	----	----	17822.781	----
147.5	----	17800.629	----	----	17822.836	----
148.5	----	17800.535	----	----	17822.891	----
149.5	----	17800.441	----	----	17822.945	----
150.5	----	17800.348	----	----	17823.004	----
151.5	----	17800.254	----	----	17823.055	----
152.5	----	17800.160	----	----	17823.109	----
153.5	----	17800.066	----	----	17823.164	----
154.5	----	17799.973	----	----	17823.219	----
155.5	----	17799.875	----	----	17823.273	----
156.5	----	----	----	----	17823.328	----
157.5	----	----	----	----	17823.383	----
158.5	----	----	----	----	17823.434	----
159.5	----	----	----	----	17823.492	----

J"	P21	P2	Q21	Q2	R21	R2
6.5	----	18568.785	----	----	----	----
7.5	18569.113	----	----	----	----	----
8.5	----	18568.617	----	----	----	----
10.5	18569.020	----	----	----	----	----
16.5	18568.844	----	----	----	----	----
37.5	----	----	----	18568.238	----	----
38.5	----	----	----	18568.207	----	----
39.5	----	----	----	18568.172	----	----
40.5	18568.074	----	----	18568.141	----	----
41.5	18568.039	----	18570.250	18568.109	18572.516	----
42.5	18568.000	----	18570.270	18568.074	18572.594	----
43.5	18567.969	18565.727	18570.289	18568.043	18572.660	18570.414
44.5	18567.934	18565.641	18570.309	18568.012	18572.734	18570.434
45.5	18567.898	18565.555	18570.328	18567.980	18572.809	18570.457
46.5	18567.863	18565.469	18570.344	18567.945	18572.875	----
47.5	18567.824	18565.383	18570.359	18567.914	18572.949	----
48.5	18567.793	18565.293	----	----	18573.020	----
49.5	18567.754	18565.207	----	18567.848	----	----
50.5	18567.723	----	----	18567.820	----	----
51.5	----	----	----	18567.785	----	----
52.5	18567.652	----	----	18567.754	----	----
53.5	18567.613	----	----	18567.719	----	----
54.5	18567.578	----	----	----	----	----